First published February 4, 2009; doi:10.1152/ajpregu.91002.2008.

Adaptive plasticity of killifish (*Fundulus heteroclitus*) embryos: dehydration-stimulated development and differential aquaporin-3 expression

Angèle Tingaud-Sequeira, Cinta Zapater, François Chauvigné, David Otero, and Joan Cerdà

Laboratory of Institut de Recerca i Tecnologia Agroalimentàries (IRTA)-Institute of Marine Sciences, Consejo Superior de Investigaciones Científicas (CSIC), Barcelona, Spain

Submitted 11 December 2008; accepted in final form 29 January 2009

Tingaud-Sequeira A, Zapater C, Chauvigné F, Otero D, Cerdà J. Adaptive plasticity of killifish (*Fundulus heteroclitus*) embryos: dehydration-stimulated development and differential aquaporin-3 expression. *Am J Physiol Regul Integr Comp Physiol* 296: R1041–R1052, 2009. First published February 4, 2009; doi:10.1152/ajpregu.91002.2008.—Embryos of the marine killifish *Fundulus heteroclitus* are adapted to survive aerially. However, it is unknown if they are able to control development under dehydration conditions. Here, we show that air-exposed blastula embryos under saturated relative humidity were able to stimulate development, and hence the time of hatching was advanced with respect to embryos continuously immersed in seawater. Embryos exposed to air at later developmental stages did not hatch until water was added, while development was not arrested. Air-exposed embryos avoided dehydration probably because of their thickened egg envelope, although it suffered significant evaporative water loss. The potential role of aquaporins as part of the embryo response to dehydration was investigated by cloning the aquaporin-0 (FhAqp0), -1a (FhAqp1a), and -3 (FhAqp3) cDNAs. Functional expression in *Xenopus laevis* oocytes showed that FhaAqp1a was a water-selective channel, whereas FhAqp3 was permeable to water, glycerol, and urea. Expression of *fhaqp0* and *fhaqp1a* was prominent during organogenesis, and their mRNA levels were similar between water- and air-incubated embryos. However, *fhaqp3* transcripts were highly and transiently accumulated during gastrulation, and the protein product was localized in the basolateral membrane of the enveloping epithelial cell layer and in the membrane of ingressing and migrating blastomers. Interestingly, both *fhaqp3* transcripts and FhAqp3 polypeptides were downregulated in air-exposed embryos. These data demonstrate that killifish embryos respond adaptively to environmental desiccation by accelerating development and that embryos are able to transduce dehydration conditions into molecular responses. The reduced synthesis of FhAqp3 may be one of these mechanisms to regulate water and/or solute transport in the embryo.

fish; desiccation; hatching; egg envelope; gastrulation; aquaporin-0; aquaporin-1; aquaporin-3

SPONTANEOUS AND REVERSIBLE arrest at specific embryonic stage is a normal aspect of the life cycle in a variety of vertebrates and invertebrates, especially those subjected to cyclic alterations of the environment (7, 38). One group of these organisms is the so-called annual fishes, a group of Cyprinodontiformes found in aquatic environments in regions of South America and Africa that dry out seasonally (39, 70). The complete drying out of this habitat leads to the death of all adult and juvenile fish, while embryos, protected from drying by a thickened egg envelope (chorion), may undergo up to three consecutive periods of diapause (developmental arrest) at distinct morphological stages (diapause I, II, or III), enabling them to survive the dry season until the rains rewet the habitat. The annual killifish *Austrofundulus limnaeus* is one of the species most studied and presents two diapause stages (II and III) (43). Diapause II embryos, which have 38–40 pairs of somites, the foundations of the central nervous system, and a functional tubular heart, exhibit a profound depression of metabolism explained in part by the arrest of protein synthesis, along with reduced water and ion permeability and an extreme tolerance to anoxia (35, 43–46).

The order Cyprinodontiformes also includes nonannual teleosts (*Cyprinodon*, *Jordanella*, *Fundulus*, *Rivulus*) with a typical teleostean development. When incubated in water under favorable conditions, eggs from these species develop continuously from fertilization to hatching. Therefore, spontaneous, prolonged, developmental arrest at stages equivalent to diapause I, II, or III apparently does not occur in these species (70), but a short-term delay or postponement of hatching which resembles diapause III of annual fishes has been described with variable frequency (28, 59, 70). During this period, embryos that reach the prehatching stage fail to hatch, remaining inside the intact chorion for periods of 1–5 wk.

The nonannual killifish *Fundulus heteroclitus* is a marine, nonmigratory teleost typically inhabiting coastal marshes and inland systems of North America (4, 33, 52), Hawaii (50), the Philippines (53) and southern Europe (23). Natural populations of *F. heteroclitus* have a semilunar reproductive cycle, coinciding with spring tide cycles that synchronize reproductive maturity and spawning with availability of specific spawning substrates that are restricted to spring tides (57). Eggs are laid in multiple clutches at the high water mark during high spring tides associated with new and full moons, usually in "protected" environments such as mussel shells or marsh chord grasses (59). The developing embryos protected by the chorion are adapted to survive aerially, and eggs laid at one high tide are ready to hatch with the next tide (59). Thus hatching occurs only on immersion in water. Early studies on the hatching mechanism of *F. heteroclitus* embryos led to the hypothesis that the level of oxygen availability may be one of the main factors regulating hatching (11, 12, 14).

Relatively isolated populations of *F. heteroclitus* from North America show slightly different hatching times, which has been related to genetic polymorphisms in heart-type lactate dehydrogenase that may affect intraerythrocyte ATP concentrations and hence hemoglobin-oxygen affinity (13, 15, 47). These studies, however, demonstrated exclusively genetic adaptations, and it is not well established whether *F. heteroclitus*

Address for reprint requests and other correspondence: J. Cerdà, Lab IRTA-ICM, CSIC, Passeig Marítim 37-49, 08003-Barcelona, Spain (e-mail: joan.cerda@irta.cat).

The costs of publication of this article were defrayed in part by the payment of page charges. The article must therefore be hereby marked "*advertisement*" in accordance with 18 U.S.C. Section 1734 solely to indicate this fact.

embryos have physiological mechanisms to regulate development in response to the environmental dehydration of the spawning sites resulting from low tides. To test this hypothesis, we have characterized the response of *F. heteroclitus* embryos to mild dehydration under laboratory-controlled conditions by determining *1*) the hatching rates, *2*) the water content in the different embryonic compartments, and *3*) the ultrastructure and biochemical composition of the egg envelope. In addition, to test the hypothesis of a potential role of aquaporins as part of the embryo response to dehydration, we identified and characterized water- and solute-permeable aquaporins and investigate their pattern of expression during embryo development.

MATERIALS AND METHODS

Fish and embryo collection. Adult killifish, *F. heteroclitus*, were obtained from saltmarshes in the bay of Cádiz (southern Spain), transported to the laboratory, and maintained as described (6). Embryos were collected daily from naturally spawning fish using plastic trays (approximately 40 × 20 × 7 cm) covered by a 3-mm net that fish use as a substrate for spawning, placed at the bottom of the tanks. Embryos were staged after Armstrong and Child (1). Procedures related to the care and use of fish were approved by the Ethics Committee of the Institut de Recerca i Tecnologia Agroalimentàries (IRTA, Spain) in accordance with the "Guiding Principles for the Care and Use of Laboratory Animals."

Embryo incubation. Groups of embryos (n = 25–30) at blastula stage, from the same batch, were placed in 60-mm Petri dishes and incubated in the dark in seawater (38‰ salinity; 1,110 mosmol/kgH_2O) or in air for 1, 3, 6, or 12 days, then transferred to dishes with seawater. The dishes were placed in sealed plastic boxes containing wet cellulose paper to maintain ~100% of relative humidity (RH). Both water-immersed and air-exposed embryos were maintained at 24–25°C in a temperature-controlled incubator up to 45 days, with the seawater changed daily. In other trials, embryos (n = 25–30) at 5, 10, or 15 days postfertilization (dpf) were incubated in air for 12 days as described above, and then transferred to seawater. In all experiments, newly hatched fry and dead embryos were recorded daily and removed. The incidence of mortality was monitored until 100% hatching. The length of the embryos was measured from head to tail, after dissecting the yolk sac, using a stereomicroscope equipped with an ocular micrometer. At least three different experiments were carried out for each developmental stage and period of air incubation, employing batches of embryos collected at different times during the year. To avoid natural variation in hatching time affecting the results, a group of embryos from the same batch in each experiment was incubated constantly in water.

Water content determination. Water content of 12 dpf intact embryos (i.e., chorion plus embryo plus yolk sac; n = 5–10), incubated in water or in air, was measured gravimetrically to constant weight at 70°C. The water content of the chorion, yolk sac, and embryo plus yolk sac was also determined separately once they were dissected out from the embryos. The water content of the perivitelline space (the compartment separating the embryo and the chorion) was then calculated indirectly.

Isolation, solubilization, and SDS-PAGE of chorion proteins. Extraction and solubilization of chorion proteins were carried out following previous protocols (45, 55) with some modifications. Chorions were manually dissected from water- and air-incubated 12 dpf embryos in cold PBS (137 mM NaCl, 2.7 mM KCl, 10 mM Na_2HPO_4, 2 mM KH_2PO_4, pH 7.4). Approximately 20 chorions were washed three times with cold PBS, centrifuged at 10,000 *g* at 4°C, and incubated in 8 M guanidine HCl, 50 mM Tris·HCl, pH 8, 5% β-mercaptoethanol, for 2 h at room temperature. Samples were heated at 100°C for 30 min and centrifuged again at 1,800 *g* for 20 min at room temperature. The supernatant was dialyzed overnight at 4°C against 10 mM NaH_2PO_4 using Slide-A-Lyzer MINI Dialysis Units (Pierce). An aliquot of the solubilized proteins was kept for determination of protein concentration using the Bio-Rad Protein assay kit, and the rest was mixed with 2× Laemmli sample buffer (32) and frozen at −80°C. SDS-PAGE of Laemmli-mixed homogenate (4 μg total protein) was run on 12% acrylamide minigels. Protein bands were visualized by PlusOne Coomassie Blue PhastGel R-350 (GE Healthcare) staining.

Cloning of F. heteroclitus aquaporins. F. heteroclitus aquaporin-0 (FhAqp0), aquaporin-1a (FhAqp1a), and aquaporin-3 (FhAqp3) cDNAs were isolated by reverse-transcriptase (RT)-PCR. Total RNA was extracted from a mixture of embryos at different developmental stages (from gastrula to somitogenesis) using the RNeasy Maxikit (Qiagen), and 10 μg was reverse transcribed using the AP primer [3′-rapid amplification of cDNA ends (3′-RACE), Invitrogen] following the manufacturer's instructions. A partial cDNA of 885 bp encoding FhAqp0, containing the COOH terminus and the complete 3′-untranslated region (UTR), was amplified using one specific forward oligonucleotide primer (5′-ACGCAGGCCCTATAAATCTGG-3′), designed according to the nucleotide sequence of the full-length FhAqp0 cDNA previously cloned (68), and the AUAP reverse primer. The 3′-end of FhAqp1a was also isolated by 3′-RACE using two forward primers (5′-GACTGATAAAAGGCGGCGTGAC-3′ and 5′-CAATCCGGCCCGGTCCTTCGG-3′) designed according to the nucleotide sequence of an expressed sequence tag (EST) deposited in GenBank (accession no. CV819692). This sequence was also employed to design two reverse primers (5′-CACTGCAATGACACACAGCA-3′ and 5′-GGCTGAGCCAAGCATTTGT-3′) to amplify the FhAqp1a 5′-end by 5′-RACE (Invitrogen). Full-length FhAqp1a was finally amplified using a forward (5′-GCAGAAGACCAGCTCCAAAG-3′) and AUAP primers and Easy-A high-fidelity DNA polymerase (Stratagene). Full-length FhAqp3 cDNA was isolated from adult gills total mRNA following the same procedure using two forward primers (5′-CCAAATCTCACCAGCCTTCA-3′ and 5′-ATGGGTCGACAGAAGATTTA-3′) designed according to the nucleotide sequence of an available EST (GenBank accession no. DN956897). In all cases, the PCR products were cloned into the pGEM-T Easy Vector (Promega) and sequenced by BigDye Terminator version 3.1 cycle sequencing on ABI PRISM 377 DNA analyzer (Applied Biosystems). The nucleotide sequences of FhAqp1a and FhAqp3 were deposited in GenBank with accession nos. EU780153 and EU780154, respectively.

Functional expression in Xenopus laevis oocytes. The FhAqp1a and FhAqp3 cDNAs were cloned into the *Eco*RV/*Spe*I sites of the oocyte expression vector pT7Ts (9). In vitro transcription of constructs, and isolation, defolliculation, and injection of *X. laevis* oocytes were as described (9). Oocytes were injected with water (control) or with 1 ng FhAqp1a cRNA or 10 ng FhAqp3 cRNA. The osmotic water permeability (P_f) was measured from the time course of osmotic oocyte swelling in a standard assay. Oocytes were transferred from 200 mosmol/kgH_2O modified Barth's medium [MBS: 88 mM NaCl, 1 mM KCl, 2.4 mM $NaHCO_3$, 10 mM HEPES, pH 7.5, 0.82 mM $MgSO_4$, 0.33 mM $Ca(NO_3)_2$, 0.41 mM $CaCl_2$, and 25 μg/ml gentamicin] to 20 mosmol/kgH_2O MBS medium at room temperature, and the swelling of the oocytes was followed under a stereomicroscope using serial images at 2-s intervals during the first 20-s period. For FhAqp3, swelling was at pH 8.5 since preliminary experiments showed maximum permeability at this pH. The P_f values were calculated as described (9). To determine glycerol permeability, water- and FhAqp3-injected oocytes were transferred to an isotonic solution containing 160 mM glycerol at pH 8.5 and adjusted to 200 mosmol/kgH_2O with MBS using a Wescor 5520 vapor pressure osmometer (Wescor). The apparent glycerol permeability coefficient (P'_{gly}) was calculated from oocyte swelling during 60 s using the equation $[d(V/V_o)/dt]/(S/V_o)$ (67), where $d(V/V_o)/dt$ is the time course change in relative oocyte volume and S is the oocyte surface area. The effect

of mercury on P_f and P'_{gly} was examined by incubating injected oocytes in MBS containing 0.3 mM $HgCl_2$ for 15 min before and during the swelling assays. To determine whether the mercurial effect was reversible, the same oocytes were rinsed three times in MBS, incubated with 5 mM β-mercaptoethanol for 15 min, and subjected to the swelling assays 2 h later. Urea transport activity mediated by FhAqp3 was measured by uptake of [^{14}C]urea (American Radiolabeled Chemicals). Injected oocytes were transferred to 1 mM urea containing 0.1 mCi/ml (52 mCi/mmol) in MBS for 10 min, rapidly rinsed three times with ice-cold MBS, and lysed in 10% SDS at room temperature followed by liquid scintillation counting.

Quantitative real-time PCR. The temporal expression pattern of *fhaqp0*, *fhaqp1a,* and *fhaqp3* mRNAs during embryo development was assessed by quantitative real-time PCR. Total RNA was extracted using the RNAeasy minikit (Qiagen) and treated with Turbo-DNase (Ambion) as indicated by the manufacturer. An aliquot corresponding to 0.5 μg was reverse transcribed using 0.5 μg oligo(dT)$_{17}$, 1 mM dNTPs, 40 IU RNase inhibitor, and 10 IU MMLuV-RT enzyme (Roche), for 1.5 h at 42°C. Real-time PCR was performed with an ABI PRISM 7900HT Sequence Detection System (Applied Biosystems) using Power SYBRGreen PCR Master Mix (Applied Biosystems). For *fhaqp0*, the forward and reverse primers were 5′-GCAGGAGACCAGGGGAGAGTC-3′ and 5′-CGCCAAACCCTCCACCTTAG-3′, respectively; for *fhaqp1a*, 5′-CAATCCGGCCCGGTCCTTCGG-3′ and 5′-CAAGAGCATAGACATATAC-3′, respectively; and for *fhaqp3*, 5′-GGTGCCCTTATTGGCACGAT-3′ and 5′-AGTCATTGGCTGCGCTTGTC-3′, respectively. In all cases, primers were located on both sides of the stop codon of the corresponding cDNAs to avoid nonspecific amplification. *F. heteroclitus* ornithine decarboxylase (*fhodc*) mRNA (GenBank accession no. CN977303) was used as a reference, employing 5′-GCTGCGTCCTCCACCTTCAT-3′ as the forward primer and 5′-GGGCATGTCCAAGCTGCTCT-3′ as the reverse primer. Amplification was in a final volume of 20 μl, containing 10 μl of the master mix, 2 μl of cDNA diluted 1:10 and 0.2 μM of each specific primer. The cycle was set as follows: activation for 120 s at 50°C and initial denaturation for 10 min at 95°C, followed by 40 cycles at 95°C for 10 s (denaturation) and 63°C for 60 s (annealing and extension). A final step, decreasing the temperature from 95°C to 60°C and increasing from 60°C to 95°C, was used to determine the melting curve. The threshold cycle number (Ct) was determined for all PCR reactions. Formation of primer dimmers was checked by adding water instead of cDNA in the reaction mixture. The relative transcript level was calculated as fold change using the $2^{-\Delta\Delta Ct}$ method (34).

Whole mount in situ hybridization. Whole mount in situ hybridization (ISH) of *fhaqp0*, *fhaqp1a,* and *fhaqp3* mRNAs in embryos was carried out as described (64). For *fhaqp0* and *fhaqp1a*, digoxigenin (DIG)-labeled sense and antisense riboprobes encoding the COOH terminus and the complete 3′-UTR were generated. For *fhaqp3*, sense and antisense riboprobes were synthesized from a cDNA fragment containing nucleotides 97 to 648 from the coding region. Prehybridization and hybridization were carried out at 62°C. After colorimetric reaction, embryos were transferred to glycerol solutions (25%, 50%, 75%, and 100%), and photos were taken of 100% glycerol-embedded embryos using a Nikon SMZ1000 stereomicroscope. Some labeled embryos were transferred to 100% ethanol, then 100% xylol, and finally embedded in paraplast (Sigma) for sectioning. Sections (14 μm) were examined and photographed with a Zeiss Axioskop 2 plus microscope.

Western blotting. Total membranes were isolated from water- and air-incubated embryos (30 embryos). Tissues were homogenized in 20 mM Tris, pH 7.4, 5 mM $MgCl_2$, 5 mM NaH_2PO_4, 1 mM EDTA, 80 mM sucrose, and cocktail of protease inhibitors (Mini EDTA-free; Roche), and centrifuged for two times 5 min each at 200 *g* at 4°C. Total membranes were isolated by a final 20-min centrifugation at 13,000 *g* at 4°C and resuspended in 0.5% SDS in PBS containing protease inhibitors. An aliquot of the homogenate was kept for determination of protein concentration, and the rest was mixed with 2× Laemmli sample buffer (32) and frozen at −80°C. For immunoblotting, 20 μg of total protein was subjected to electrophoresis on 12% SDS-PAGE. Proteins were blotted on Amersham Hybond ECL membranes (GE Healthcare) in high-glycine transfer buffer (190 mM glycine, 250 mM Tris, pH 8.6, and 20% methanol). Membranes were blocked for 1 h at room temperature in 5% nonfat dried milk in Tris-buffered saline with 0.1% Tween and incubated overnight (1:100) with FhAqp3 rabbit affinity-purified antisera. The antisera was raised against a synthetic peptide corresponding to the COOH termini of FhAqp3 (SLQLTINANGKEAN). Bound antibodies were detected with goat anti-rabbit IgG antibodies (1:8,000) coupled to horseradish peroxidase using enhanced chemiluminescence (Amersham ECL, GE Healthcare). Control membranes were incubated with the antisera preadsorbed with a 30-fold molar excess of the immunizing peptide.

Immunofluorescence microscopy. Chorion-bearing gastrula embryos were permeabilized with 3% NaOCl for 1 min and fixed with 4% paraformaldehyde (PFA) in PBS for 4 h at room temperature, manually dechorionated, and refixed with 4% PFA for 1 h. Embryos were then dehydrated and embedded in Paraplast (Sigma). Sections (15 μm) were blocked with 5% goat serum in PBST (0.1% BSA and 0.01% Tween 20 in PBS) for 1 h, and incubated with FhAqp3 antisera (1:100) in PBST with 1% goat serum overnight at 4°C. After washing with PBS, the sections were incubated with fluorescein isothiocyanate anti-rabbit secondary antibodies (1:300 in PBS) for 1 h, washed three times with PBS, and mounted with ProLong Gold antifade reagent (Molecular probes). Control sections were incubated with the antisera previously incubated with the corresponding synthetic peptides as described above, or with the preimmune sera (data not shown). In both cases, no positive staining was observed. Immunofluorescence was observed and documented with a Leica SP2 confocal microscope.

Electron microscopy. Chorions dissected from 12 dpf embryos incubated in water or in air were fixed in 2.5% glutaraldehyde in seawater for 13 h at room temperature and then washed in seawater for 2 h. The chorions were transferred to seawater containing 2% osmium tetroxide for 2 h, washed in seawater for 1.5 h, and incubated in 20% ethanol for 20 h at 4°C. Samples were progressively dehydrated to 100% ethanol, and transferred progressively to 100% acetone. Finally, the samples were subjected to critical point drying using carbon dioxide and a POLARON CA508 evaporator (Quorum Technologies). Samples were examined with a Hitachi S-570 scanning electron microscope.

Statistical analysis. Data are presented as means ± SE. Linear data on the hatching percentage vs. time for each trial and experimental group were considered to estimate the time of 50% hatching using the equation $y = ax + b$. The Student's *t*-test was used to compare the time for 50% hatching between treatments, as well as embryo length and water content. Aquaporin mRNA expression levels were analyzed by two-factor ANOVA followed by Tukey's multiple-range test. In all analyses, differences were considered significant at $P < 0.05$.

RESULTS

Water removal and embryo development. To determine the effect of dehydration on *F. heteroclitus* embryo development, blastula embryos collected from different batches obtained during the year were incubated in seawater (control) or in air for 1, 3, or 6 days and subsequently transferred to seawater (Fig. 1). Hatching was recorded daily until 100% hatching was observed. Different batches of control embryos showed some variation in the day of 50% hatching, although not statistically significant (Table 1), and air incubation for 1 or 3 days did not affect the hatching time compared with controls (Fig. 1, *A* and *B;* Table 1). However, embryos incubated in air for 6 days started to hatch before the control group and reached 100% hatching some days earlier than control embryos (Fig. 1*C*), with 50% hatching ~3 days before control embryos (Table 1).

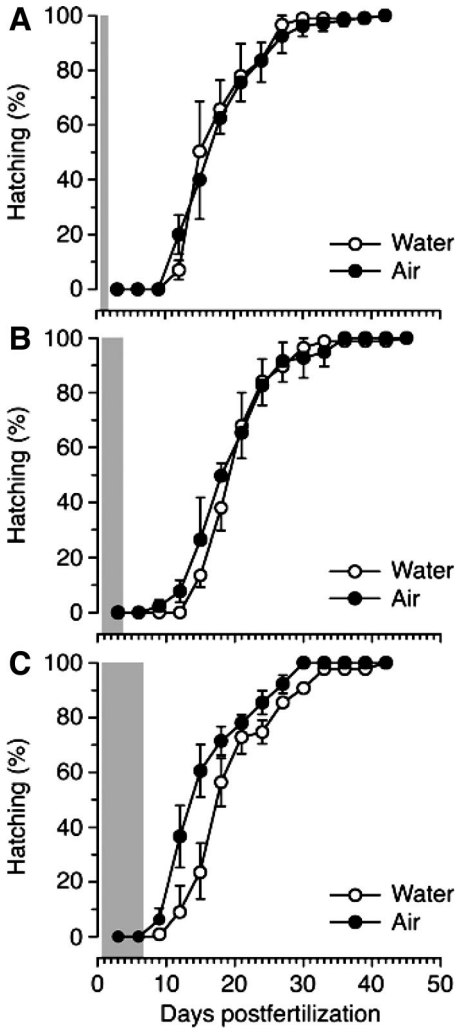

Fig. 1. Effect of dehydration on percentage hatching of *Fundulus heteroclitus* embryos. Groups of embryos (n = 25–30) at blastulae stage were incubated with or without seawater for 1 (*A*), 3 (*B*), or 6 (*C*) days and subsequently transferred to seawater. Hatching of water- and air-incubated embryos was recorded daily. Data are means ± SE (n = 3 experiments). The gray bars in each panel indicate the duration of the air exposure period.

To investigate whether embryos were able to control hatching time during development, a series of experiments were carried out in which embryos at blastula (Fig. 2*A*) and at 5 (Fig. 2*B*), 10 (Fig. 2*C*), and 15 dpf (Fig. 2*D*) were incubated in air for 12 days and subsequently transferred to seawater. After 12 days of air exposure, with blastula-stage embryos, 50% hatching was ~10 days earlier than in controls (Fig. 2*E*; Table 2), earlier than that observed previously after 6 days of air incubation. With 5 dpf embryos, hatching was advanced by 7 days with respect to the controls (Fig. 2*F*; Table 2). In contrast, hatching was not advanced in 10 and 15 dpf embryos incubated in air (Table 2), with embryos hatching on the day water was added or 1 day later, indicating that most embryos awaited water to hatch (Fig. 2, *G* and *H*). Interestingly, ~15% of embryos of these two groups started to hatch toward the end of the 12-day incubation period without water.

The mortality rate was similar in all the treatments (~28%), suggesting that exposure of embryos to air for up to 12 days was not deleterious (data not shown). On the contrary, the developmental rate of air-incubated embryos was enhanced with respect to embryos maintained in water, which could explain the earlier hatching times. On measuring the length of embryos after incubation in air or water for 1, 3, 6, and 12 days (Fig. 3), we found that, after 6 and 12 days, overall growth and differentiation was enhanced in embryos incubated in air, being longer (Fig. 3*A*), with a smaller yolk sac, more developed eye and jaws, and increased body pigmentation (Fig. 3*B*), than those incubated in water.

Water content of embryos. The water content of 12 dpf embryos (plus chorion) incubated in water or air from the blastulae stage, under ~100% RH, remained unchanged (Table 3), indicating that *F. heteroclitus* embryos survive periods of exposure to air by completely avoiding water loss. However, there were some differences in the water content of embryonic compartments isolated by manual dissection, i.e., chorion, embryo plus yolk sac, and yolk sac. Air-incubated embryos appear to retain less water in the chorion than water-incubated embryos but had more water in the embryo plus yolk compartment. Since both wet and dry weight of the yolk sac were lower in air-incubated embryos, but with similar overall water content, it seems that water in the embryo comes from the yolk sac, probably as a result of faster consumption of yolk due to enhanced growth. Calculations indicated that the perivitelline space of air-incubated embryos loses some water, but the differences with respect to controls were not statistically significant (Table 3).

Ultrastructural analysis of macroscopic changes in the chorion following water removal, using scanning electron microscopy, revealed that in *F. heteroclitus* air-incubated embryos the acellular layers of the egg envelope were not as closely packed as in water-immersed embryos, thus resulting in a thicker chorion (data not shown). In addition, the outer layers of the egg envelope of air-exposed embryos revealed a fibrillar structure, possibly caused by the loss of water as observed before, while the inner layers had the same structural aspect as those of embryos maintained in water. Biochemical analysis of egg envelope proteins by SDS-PAGE revealed the presence of seven major protein bands in water-incubated embryos, whereas in embryos dehydrated for 12 days some of these bands were completely absent, while new bands of smaller molecular mass appeared (data not shown).

cDNA cloning and functional expression of FhAqp1a and FhAqp3. To investigate the potential regulation of aquaporin expression in *F. heteroclitus* embryos exposed to air, we cloned the cDNAs encoding two water-selective aquaporins, FhAqp0 and FhAqp1a, as well as one aquaglyceroporin (water-

Table 1. *Day of 50% hatching of Fundulus heteroclitus embryos incubated continuously in seawater or exposed to air for 1, 3, or 6 days from the blastula stage*

	Time of Air Exposure		
	1 day (n = 3)	3 days (n = 3)	6 days (n = 3)
Water incubated	14.8±0.1	17.4±1.3	18.3±1.2
Air incubated	14.5±0.5	15.8±1.1	14.8±0.1*

Values are means ± SE (n = 3 different experiments using different batches of embryos; n = 25-30 embryos per treatment). *Data from air-incubated embryos are statistically different ($P < 0.05$; Student's t-test) from those of embryos incubated in seawater.

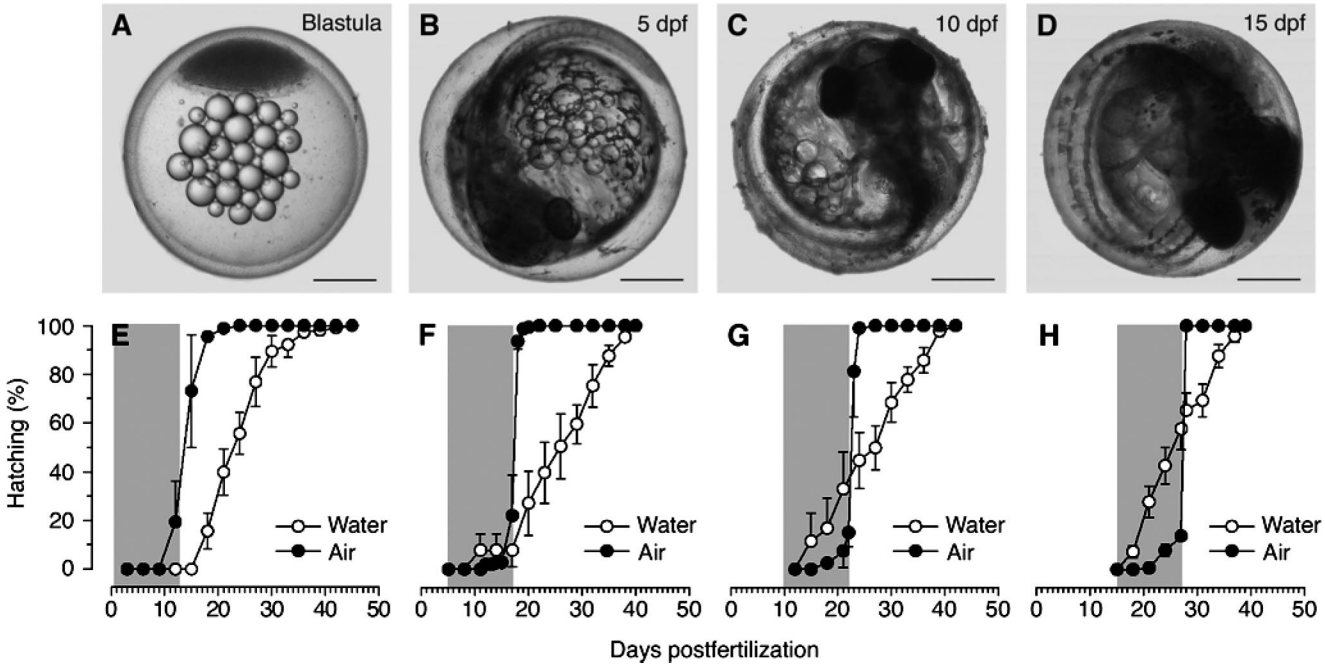

Fig. 2. Effect of dehydration on percentage hatching in *F. heteroclitus* embryos at different stage of development. Groups of embryos (n = 25–30) at blastulae stage (*A*) and 5 (*B*), 10 (*C*), and 15 days postfertilization (dpf) (*D*) were incubated with or without seawater for 12 days and subsequently transferred to seawater. Scale bars, 500 μm. Hatching (*E–H*) in each group was recorded daily. Data are means ± SE (n = 3 experiments). The gray bars in each panel indicate the duration of the air exposure period.

and solute-permeating aquaporin), FhAqp3. The FhAqp1a cDNA was 1,277 nucleotides long encoding a predicted protein of 261 amino acids with six potential transmembrane domains and two highly conserved Asn-Pro-Ala (NPA) motifs, the hallmark of the membrane intrinsic protein (MIP) family to which aquaporins belong (31). The deduced amino acid sequence of this cDNA shared 74–76% identity with mammalian AQP1, and 91–96% and 55–62% identity with Aqp1a and Aqp1b sequences, respectively, from other teleosts (see Supplemental Fig. 1S*A*, available with the online version of this article). In addition, the FhAqp1a amino acid sequence included the residues of the pore-forming region (Phe^{50}, His^{172}, and Arg^{187}) conserved in water-selective aquaporins (56), as well as the Cys residue before the second NPA motif (Cys^{181}), which is the site potentially responsible for the inhibition of water permeability by mercurial compounds (49).

The FhAqp3 cDNA was of 2,175 nucleotides with a very long UTR of 1,262 nucleotides, including two AATAAA polyadenylation signals. The nucleotide sequence encoded a predicted protein of 295 amino acids that shared 77–79% and 82–96% identity with mammalian and teleost AQP3 sequences, respectively (see Supplemental Fig. 1S*B*, available with the online version of this article) but only 62–69% with other aquaglyceroporins. In addition to the six putative transmembrane domains and the two NPA motifs, the FhAqp3 amino acid sequence had the five amino acid positions P1 (aromatic), P2 (Asp), P3 (Lys or Arg), P4 (Pro), and P5 (nonaromatic), i.e., Tyr^{122}, Asp^{217}, Arg^{221}, Pro^{244}, and Leu^{245}, conserved in mammalian AQP3 and other aquaglyceroporins (21). A Cys residue close to the second NPA motif was not present, but a Cys was found in loop B preceding the first NPA motif (Cys^{73}) as observed in eel (8) and sea bass (22) Aqp3 amino acid sequences.

Table 2. *Day of 50% hatching of F. heteroclitus embryos incubated continuously in seawater or exposed to air for 12 days from blastula or 5, 10, or 15 dpf*

	Blastulae (n = 4)	5 dpf (n = 4)	10 dpf (n = 4)	15 dpf (n = 4)
Water incubated	22.9±1.4	24.7±2.6	25.6±2.7	25.2±1.5
Air incubated	12.4±0.2†	17.9±0.3*	23.0±0.3	27.7±0.0

Values are means ± SE (n = 4 different experiments using different batches of embryos; n = 25-30 embryos per treatment). dpf, days postfertilization. Data from air-incubated embryos statistically different from those of embryos incubated in seawater: *$P < 0.05$; †$P < 0.01$ (Student's t-test).

To confirm that both FhAqp1a and FhAqp3 cDNAs encoded functional channels, *X. laevis* oocytes injected with FhAqp1a (1 ng) or FhAqp3 (10 ng) cRNAs were compared with control oocytes injected with 50 nl of water (Fig. 4). Coefficients of P_f and P'_{gly} were determined from rates of oocyte swelling after transfer to hyposmotic MBS (P_f) or isotonic MBS with 160 mM glycerol (P'_{gly}). Water-injected oocytes exhibited low water permeability, whereas the P_f of FhAqp1a (Fig. 4*A*) and FhAqp3 (Fig. 4*B*) oocytes increased by 14.4- and 3.4-fold, respectively. In the presence of 0.3 mM $HgCl_2$, the P_f of FhAqp1a- and FhAqp3-injected oocytes was reduced by 93% and 100%, respectively. Mercury inhibition was completely or partially recovered by incubation of oocytes with β-mercaptoethanol. FhAqp3 oocytes, but not FhAqp1a oocytes (data not shown), showed a 12.1-fold increase in P'_{gly} with respect to controls, which was also 97% inhibited by mercury and almost completely recovered with β-mercaptoethanol (Fig. 4*C*). Radiotracer methods also demonstrated that FhAqp3 was permeated by urea (Fig. 4*D*).

Differential aquaporin expression during embryo development. The expression pattern of *fhaqp0, fhaqp1a,* and *fhaqp3* during development in water- and air-incubated embryos was

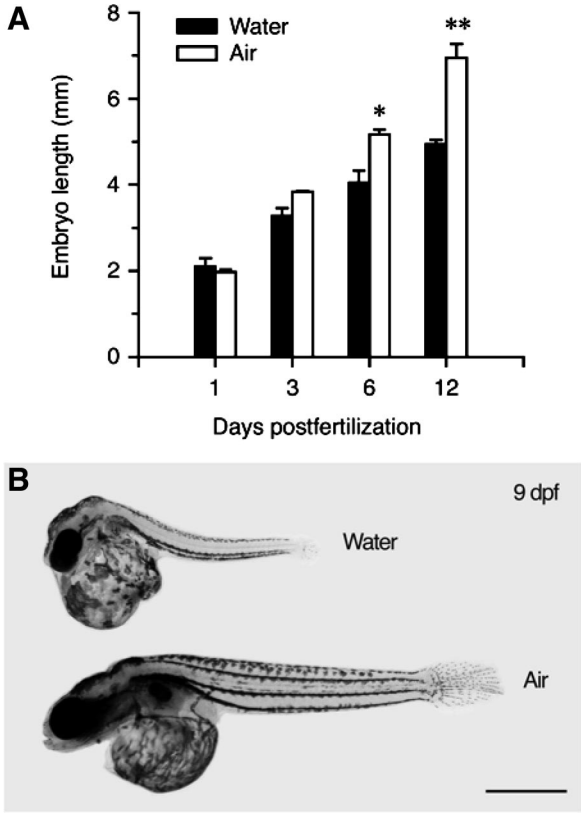

Fig. 3. Effect of dehydration on *F. heteroclitus* embryo development. *A*: length of embryos incubated in seawater or air, for 1, 3, 6, and 12 days from the blastulae stage. Data are means ± SE ($n = 3$ experiments). *B*: photomicrograph of water- and air-incubated embryos after 9 days. Scale bar, 500 μm. $*P < 0.05$, $**P < 0.01$ vs. water-exposed embryo at same time point.

investigated by whole mount ISH (Fig. 5) and real-time PCR (Fig. 6). Transcripts of *fhaqp0* were first and exclusively detected in the lens of the developing eye at late neurula stage (Fig. 5, *A* and *B*). Using real-time PCR, the expression of *fhaqp0* in air-incubated embryos was detected earlier than in control embryos, in agreement with their enhanced growth and differentiation, and the mRNA levels remained higher than in controls until the 28-somites stage (Fig. 6*A*).

In contrast, the expression of *fhaqp1a* was detected by real-time PCR in the 2- to 4-cells stage (Fig. 6*B*). Using ISH, however, the mRNA was not observed until the onset of somitogenesis, where it was expressed in the caudal artery (Fig. 5*C*), the primitive internal carotid artery, and in the primordial midbrain channel (Fig. 5*D*). At later stages, *fhaqp1a* expression in blood vessels became stronger as the caudal artery and the intersegmental vessels developed during somitogenesis (Fig. 5, *E–G*). Real-time PCR confirmed a progressive increase of *fhaqp1a* mRNA levels from the 2- to 4-cells stage up to the 28-somites stage, with no differences between water- and air-incubated embryos (Fig. 6*B*).

Transcripts encoding *fhaqp3* were first noted at the onset of gastrulation widely detected in the blastoderm, although some blastomers were more intensely labeled than others (Fig. 5, *H* and *I*). With the progression of epiboly, the *fhaqp3* signal became more intense in the marginal region of the blastoderm containing migrating cells of the germ ring (Fig. 5*J*). By the end of gastrulation, *fhaqp3* expression was no longer detected. By 4 dpf, *fhaqp3* transcripts were detected again in specific cells of the epidermis of the dorsal area (Fig. 5*K*), and by 7 dpf, transcripts were also prominent in the caudal fin bud (Fig. 5, *L* and *M*), as well as in cells of the pectoral fins (not shown). Real-time PCR confirmed the specific expression pattern of *fhaqp3* during gastrulation, indicating a major increase in mRNA levels at the beginning and end of epiboly, and a further decrease to almost undetectable levels (Fig. 6*C*). Interestingly, although both water- and air-incubated embryos had increased *fhaqp3* mRNA levels during the midblastula transition, accumulation of *fhaqp3* transcripts was lower in air-incubated embryos than water-incubated embryos at later stages of gastrulation.

Cellular localization of FhAqp3 in gastrula embryos and effect of air exposure on protein abundance. The cellular distribution of FhAqp3 in water-immersed gastrula embryos at ~50% epiboly was characterized by immunofluorescence light microscopy using a rabbit affinity-purified antisera. In the animal pole of embryos (Fig. 7*A*), FhAqp3 immunoreactivity was detected in the basolateral membrane of the cells of the enveloping layer (EVL), the outermost epithelial cell layer of the blastoderm, whereas the yolk syncytial layer (YSL) was negative (Fig. 7*B*). In the marginal zone of the blastoderm (Fig. 7*A*), where internalization of blastomers via ingression and further migration of cells toward the animal pole occur (51, 66), overall FhAqp3 immunofluorescence increased and appeared to be localized at the membrane of the EVL cells as well as in some migrating blastomers (Fig. 7*C*). These data were thus consistent with the increased accumulation of *fhaqp3* transcripts at the marginal blastoderm during epiboly previously observed.

To investigate whether exposure of embryos to air was able to reduce the levels of FhAqp3 protein during gastrulation,

Table 3. *Water content of F. heteroclitus embryos continuously immersed in seawater or exposed to air for 12 days from the blastula stage*

	Water Incubated	Air Incubated
Whole embryo		
Wet weight, mg	4.10±0.01	4.34±0.08
Dry weight, mg	0.89±0.04	0.89±0.00
Water weight, mg	3.21±0.03	3.45±0.01
%Water	78.32±0.98	79.46±0.47
Chorion		
Wet weight, mg	0.23±0.03	0.22±0.02
Dry weight, mg	0.20±0.02	0.21±0.02
Water weight, mg	0.02±0.004	0.01±0.002*
%Water	9.42±0.73	4.78±0.35*
Embryo plus yolk sac		
Wet weight, mg	1.22±0.15	2.42±0.14*
Dry weight, mg	0.40±0.05	0.62±0.06*
Water weight, mg	0.83±0.07	1.80±0.08*
%Water	68.33±1.93	74.54±1.13*
Yolk sac		
Wet weight, mg	0.46±0.04	0.23±0.02*
Dry weight, mg	0.27±0.04	0.14±0.02*
Water weight, mg	0.19±0.03	0.23±0.02
%Water	41.89±6.25	37.23±2.23
Perivitelline space		
%Water	23.08±2.86	19.91±0.75

Values are means ± SE (n = 3-5 different experiments using different batches of embryos). *Data from air-incubated embryos are statistically different ($P < 0.05$; Student's t-test) from those of embryos incubated in seawater.

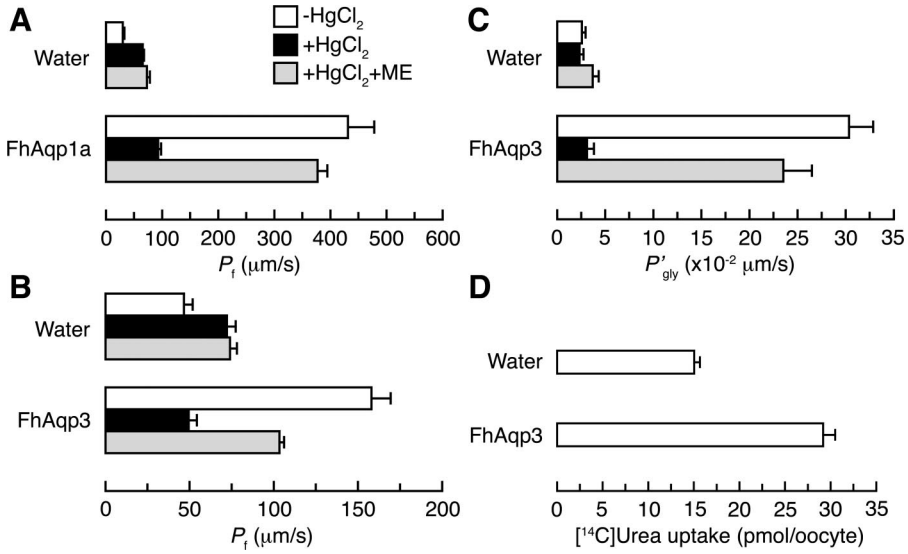

Fig. 4. Functional characterization of FhAqp1 and FhAqp3 in *Xenopus laevis* oocytes. Osmotic water permeability (P_f; *A* and *B*), apparent glycerol permeability (P'_{gly}; *C*), and urea uptake (*D*) of *X. laevis* oocytes expressing FhAqp1 (*A*) or FhAqp3 (*B–D*) are shown. Oocytes were injected with cRNAs encoding FhAqp1a (1 ng) or FhAqp3 (10 ng), or with 50 nl of water (control). The P_f and P'_{gly} were assayed in the presence or absence of 0.3 mM $HgCl_2$. Some oocytes treated with $HgCl_2$ were incubated with 5 mM β-mercaptoethanol (ME) for 15 min before swelling measurements. Urea transport activity was measured by [^{14}C]urea uptake. Values are means ± SE (n = 6–10 oocytes) from a representative experiment.

Western blotting analysis was performed employing the same antisera and purified cell membrane fractions isolated from water- and air-exposed embryos (Fig. 7*E*). Immunoblotting showed a single protein band with a molecular mass of ~32 kDa in extracts from water-immersed embryos, thus being consistent with the molecular mass of FhAqp3 (32.1 kDa) calculated from the deduced amino acid sequence of its cDNA (Fig. 7*E*, *left*). In extracts from air-exposed embryos, the 32-kDa band was less intense, suggesting that in these embryos the synthesis of FhAqp3 was reduced although not completely abolished (Fig. 7*E*, *left*). Control blots incubated with the FhAqp3 antisera preadsorbed with large amounts of the immunizing peptide were negative (Fig. 7*E*, *right*), indicating the specificity of the reaction.

DISCUSSION

Air exposure as a developmental cue in F. heteroclitus embryos. Earlier field studies have shown that *F. heteroclitus* spawns around the time of high tides in a few centimeters of water at the high-water level. Embryos are stranded in air for large portions of their developmental period, and hatching occurs by immersion in water with subsequent high tides (59–61). It has been suggested that the respiratory demands of developing embryos are fulfilled by the oxygen supply from the air, whereas hatching is cued when the metabolic rate of the embryo exceeds a limit set by the diffusion of oxygen through the water column (13–15, 47).

The present study shows that air-exposed *F. heteroclitus* embryos not only survive, but accelerate development, with respect to continuously immersed embryos. Blastula embryos are able to resist dehydration up to 12 days under ~100% RH (in this study), hatching 1–2 days after water addition. The time for 50% hatching is 4–10 days in advance of water-incubated embryos, depending on the exposure time to air. Such ability of blastula embryos to accelerate development in response to water removal may be maternally inherited, since zygotic transcription is possibly not yet activated at this embryonic stage (41). The observation that 2- to 4-cell embryos show the same response to environmental dehydration as blastula embryos supports this view (data not shown).

In contrast to air-exposed embryos, constant immersion in water caused a delay in hatching. A delayed hatching or failure to hatch of *F. heteroclitus* embryos exposed to continuous immersion, or daily immersion by flood tides, has been described in field experiments (60) and in embryos maintained in the laboratory without change of water (29, 61). As water was changed daily in this study, delayed hatching of water-incubated embryos was possibly related to decreased oxygen availability by continuous immersion in water when compared with air-exposed embryos. However, we also observed large variations in hatching times between batches of embryos collected during the year that were incubated constantly in water. In addition, we found that incubation of embryos in seawater with reduced salinity (15–19‰) also accelerated development (data not shown). Therefore, these observations suggest that oxygen availability may not be the only environmental cue controlling the developmental rates.

The present and earlier studies suggest that *F. heteroclitus* embryos are adapted to their specific reproductive strategy. During the reproductive season, gonad maturity and spawning readiness coincide with new and full moons, and spawning is thereby synchronized with the semilunar cycle of tides in the tidemarsh habitat (59, 62). By the accelerated development of embryos deposited during the high tide, which are later exposed to air, the ability of embryos to hatch during the next high tide is increased (59). In the laboratory, the lunar and tidal spawning cycles of parent fish may be partially lost (25–27, 58), but, as shown here, the ability of embryos to accelerate development in response to dehydration is conserved. This strategy resembles that of tadpoles of desert-dwelling amphibians, which are able to detect changes in the water level of the aquaria and accelerate development and metamorphosis, mimicking their behavior in the natural habitat (10).

Mechanisms for water retention. Some aquatic vertebrates and soil-dwelling arthropods have mechanisms for preventing water loss when faced with desiccation conditions (3, 20, 37, 69), although they are only effective under mild or moderate dehydration stress (>98% RH). In the annual killifish *A. limnaeus*, embryos can avoid water loss up to 85% RH, but only diapause II embryos can retain water and survive up to

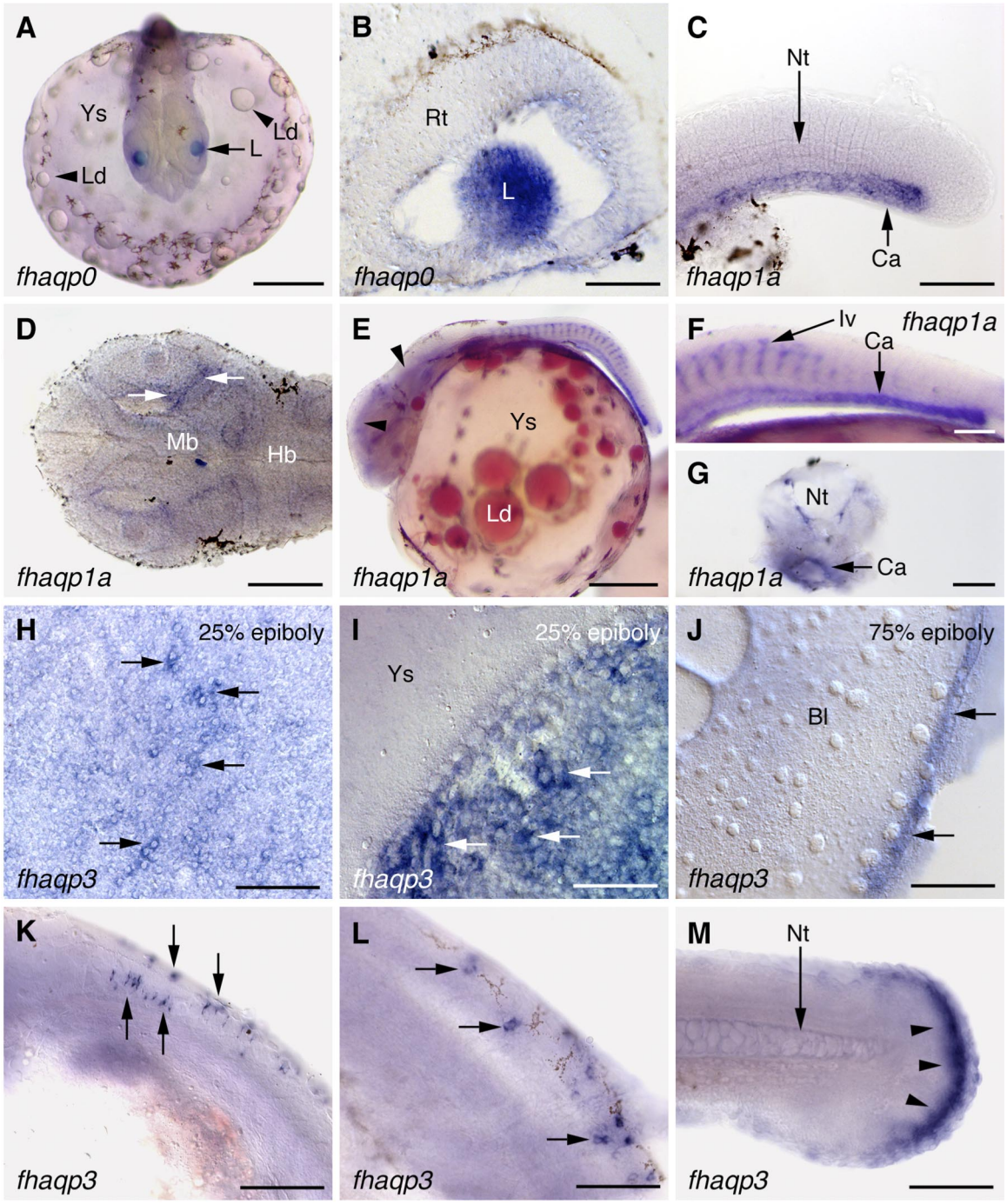

Fig. 5. Expression of *fhaqp0*, *fhaqp1a,* and *fhaqp3* in embryos by whole mount in situ hybridization using antisense DIG-labeled riboprobes. Lateral (*A–C, E, F, K–M*) and dorsal (*D, H–J*) views with rostral to the left, and 10-μm cross section (*B, G*). *A* and *B*: specific expression of *fhaqp0* in the lens (L) of a late neural embryo, lacking in the retina (Rt). Lipid droplets (Ld) in the yolk sac (Ys) are indicated by arrowheads. *C*: expression of *fhaqp1a* in likely differentiating cells of the caudal artery (Ca) under the developing notochord (Nt) in 36-h postfertilization embryos. *D*: weak *fhaqp1a* expression in the presumptive internal carotid artery in the midbrain (Mb, arrows). Hb, hindbrain. *E–G*: at 2 dpf, *fhaqp1a* expression in the developing blood vessels along the embryonic body was more prominent (arrowheads in *E*), including the intersegmental vessels (Iv) surrounding the somites (*F*). *H* and *I*: expression of *fhaqp3* in cells of the blastoderm (arrows) during early gastrulation (25% epiboly). *J*: *fhaqp3* highly expressed in the marginal region of the blastoderm (Bl) (arrows) by ~75% epiboly. *K*: *fhaqp3* transcripts were not detected again until 4 dpf, when they appeared in specific, nonidentified cells of the epidermis (arrows). *L*: expression of *fhaqp3* in epidermal cells at 7 dpf (arrows). *M*: expression of *fhaqp3* in the caudal fin bud (arrowheads) of 7 dpf embryos. Scale bars, 500 μm (*A, E, H–M*); 250 μm (*F* and *G*); and 100 μm (*B–D*).

50% RH (45). Although *F. heteroclitus* embryos did not enter into diapause under the conditions tested, as indicated by the rapid hatching of air-exposed embryos following water addition, they were able to retain the water in the whole embryo at 100% RH. Whether they are able to retain water and survive at lower RH is not known.

In *A. limnaeus*, the egg envelope may be the major barrier to prevent lethal dehydration of the embryo (45). A similar

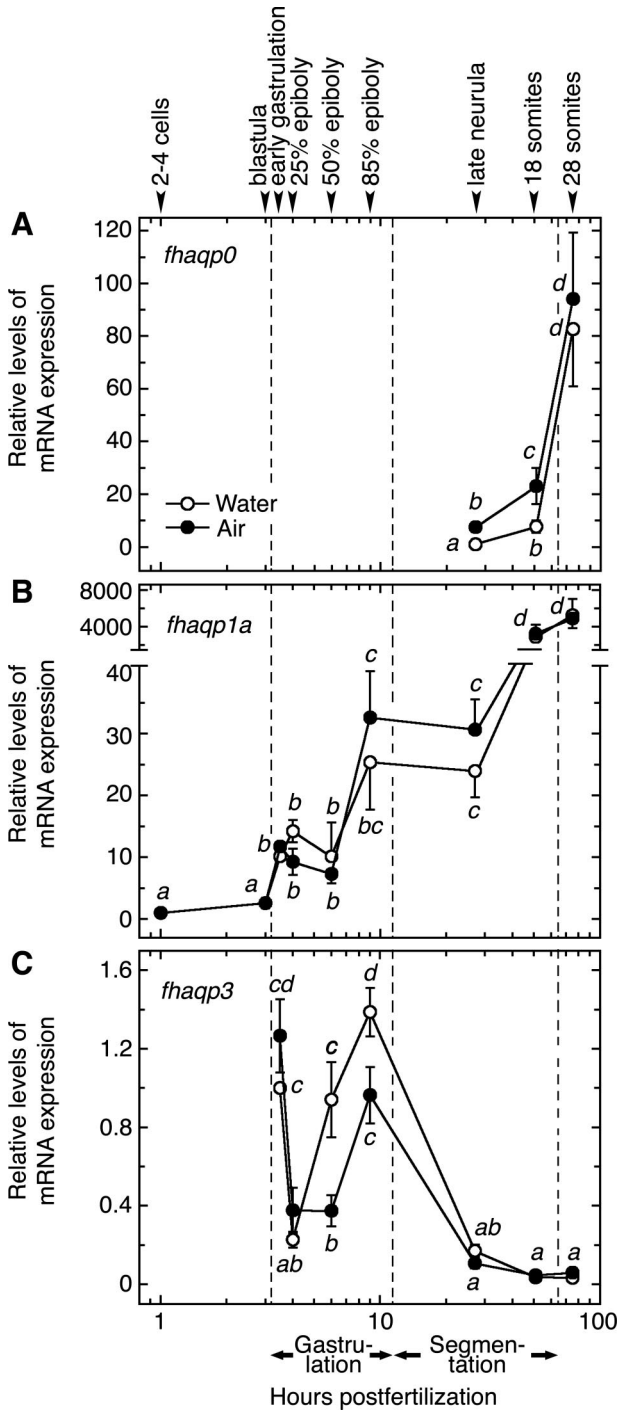

Fig. 6. Developmental expression of *fhaqp0* (*A*), *fhaqp1a* (*B*), and *fhaqp3* (*C*) genes in embryos kept in water or air as determined by real-time PCR. The transcript level of *fhodc* was used as a reference, and relative transcript levels were calculated as fold change. Data are presented as means ± SE ($n = 3$ different cDNAs from different batches of embryos). Values with different superscript letter (*a, b, c, d*) in each panel are significantly different (ANOVA, $P < 0.05$).

situation is suggested for *F. heteroclitus* embryos exposed to air since water evaporated only from the chorion, whereas the water of the embryonic/yolk compartment was retained. However, in *A. limnaeus* diapause II and *F. heteroclitus* embryos, the egg envelope may not be solely responsible for resistance to water loss, as this layer is not completely impermeable (30, 54) and its structure does not change in embryos at different diapause stage (45) or between water- and air-incubated embryos. Therefore, mechanisms other than changes in the egg envelope proteins may be involved in the ability of *A. limnaeus* and *F. heteroclitus* embryos to avoid complete dehydration. Podrabsky et al. (45) have proposed that one mechanism might be the secretion of substances into the perivitelline space to prevent water loss by creating a hydrophobic barrier or by allowing vitrification. Although this mechanism has not been yet demonstrated in fish embryos, recent microarray analyses have revealed the accumulation of certain sugar-binding lectin mRNAs in air-incubated *F. heteroclitus* embryos (Tingaud-Sequeira and Cerdà, unpublished data).

Aquaporin expression. Water determination in the different embryonic compartments of *F. heteroclitus* suggested that under air exposure, water required for development is probably obtained from the yolk compartment along with the mobilization of nutrients. This led us to hypothesize a potential role of aquaporins during this process, since these membrane proteins are involved in water transport in different tissues and cell types in all organisms (31). To investigate this, we isolated the cDNAs encoding FhAqp0, FhAqp1a, and FhAqp3 and determined their spatial and temporal expression pattern during embryo development in the presence and absence of water. Virkki et al. (68) recently showed that FhAqp0 cDNA encodes a water-selective aquaporin when artificially expressed in *X. laevis* oocytes, although it is also weakly permeable to CO_2 as mammalian AQP1 (18). In adult fish, *fhaqp0* is specifically expressed in the ocular lens (68), and we found that embryos start to accumulate *fhaqp0* transcripts in the lens at the neurula stage. Since overall development was accelerated in air-incubated embryos, the *fhaqp0* mRNA levels were higher in these embryos than in water-immersed embryos. The differential *fhaqp0* expression between water- and air-incubated embryos is probably due to the different progression of eye and lens differentiation in both groups. In mammals, mature lens fiber cells express a large amount of AQP0 protein (5), and it is believed that this aquaporin mediates fluid and nutrient circulation in the avascular lens (36). In fish, although the specific functions of Aqp0 are not known, it is probable that it is also involved in mediating efficient fluid circulation in the lens (68).

In teleosts, two AQP1-like channels, Aqp1a and Aqp1b, have recently been identified (65). The AQP1-like cDNA that we isolated from *F. heteroclitus* is likely to encode the teleost Aqp1a ortholog, since its predicted amino acid sequence showed the highest identity to mammalian AQP1 and teleost Aqp1a. In addition, functional expression in oocytes demonstrated that FhAqp1a was permeable only to water and sensitive to mercury, which are typical characteristics of mammalian AQP1 (48). In embryos, the expression of *fhaqp1a* was prominent in the caudal artery and intersegmental blood vessels during somitogenesis. Such specific staining is consistent with the presence of AQP1 in endothelial cells lining continuous capillaries of a variety of tissues, where it plays a role in transepithelial water transport (40). The *fhaqp1a* transcript levels were similar in water- and air-incubated embryos, which suggests that organogenesis was not affected by air exposure.

Amino acid sequence analysis of FhAqp3 identified aquaglyceroporin-distinctive residues at key locations, as well as a higher identity to vertebrate AQP3, indicating that FhAqp3 is

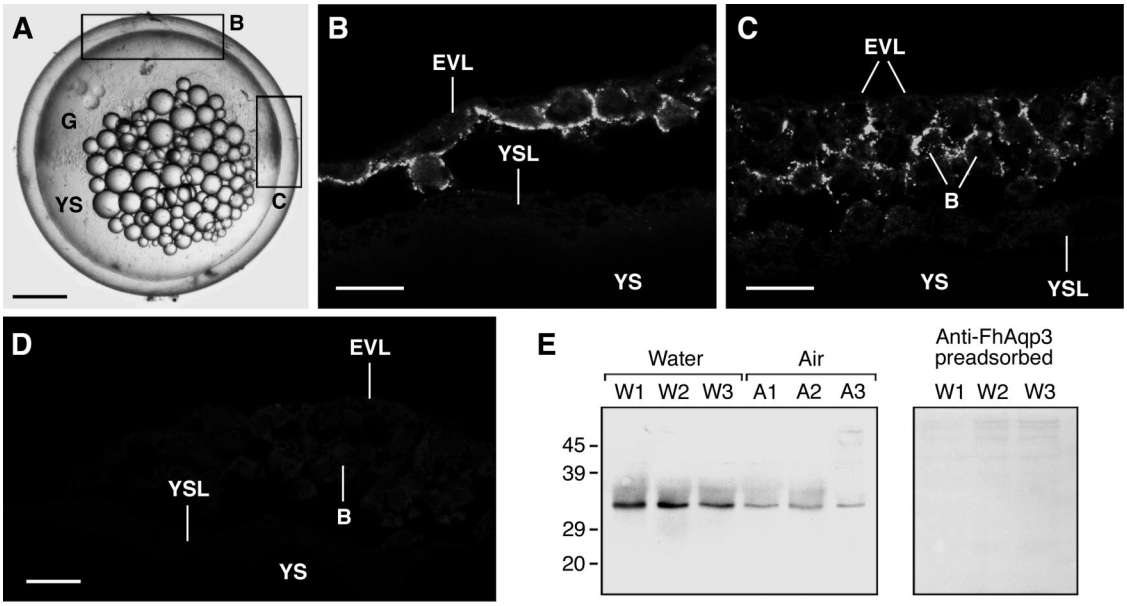

Fig. 7. Immunolocalization of FhAqp3 in *F. heteroclitus* gastrula embryos and effect of air-exposure on FhAqp3 abundance. *A*: photomicrograph of a midgastrula embryo. *B–D*: immunofluorescence microscopy on paraffin sections from gastrula embryos (*B* and *C* correspond to the regions indicated in *A*, and *D* shows a control section incubated with antigen-negated FhAqp3). *E*: representative Western blot of protein extracts (20 μg) of total membranes from water (W)- and air (A)-incubated embryos ($n = 3$ different batches) during gastrulation. Blots were incubated with anti-FhAqp3 (*left*) or with anti-FhAqp3 preadsorbed with the synthetic peptide (*right*). The apparent molecular masses (kDa) are indicated on the left. G, gastrula; EVL, enveloping layer; YSL, yolk syncytial layer; YS, yolk sac; B, blastomers. Bars, 25 μm.

the AQP3 ortholog. This conclusion is supported by the finding that FhAqp3 was permeable to water, glycerol, and urea when expressed in oocytes. In embryos, we found that expression of *fhaqp3*, unlike that of *fhaqp0* and *fhaqp1a*, occurred transiently from the midblastula transition through gastrulation, and at later stages expression was noted again in the skin and in the fin bud, which agrees with the known presence of AQP3 in mammalian epidermis (24). During gastrulation, the *fhaqp3* transcripts were initially widely distributed in the blastoderm, but as epiboly progressed they were more prominent at the marginal region. Immunolocalization experiments confirmed the expression of FhAqp3 and revealed the presence of the protein in the basolateral membrane of the cells of the EVL. These observations are consistent with those previously reported in zebrafish (*Danio rerio*) for the mRNA of one of the Aqp3 isoforms (63), as well as in mouse embryos where AQP3 polypeptides are present in the apical side of morula blastomers and in basolateral membranes of trophectodermal epithelial cells of blastocysts (2, 17).

In teleosts, gastrulation occurs by the epiboly of the EVL and YSL, followed by the internalization of cells at the marginal zone and subsequent migration toward the animal pole (51). The specific localization of FhAqp3 in the EVL may indicate that this channel is required for water and/or solute transport during epiboly, although early studies in *F. heteroclitus* midgastrula embryos reported low water permeability of the EVL (16). The high level of *fhaqp3* and FhAqp3 expression at the blastoderm margins could be related to the increased plasma membrane turnover of the EVL cells necessary to increase the surface area of the epithelia during epiboly (19, 51). However, in this region of the blastoderm we also detected strong FhAqp3 immunostaining in the membrane of internalizing and possibly migrating blastomers. Such characteristic staining might point to an involvement of FhAqp3 in cell migration during gastrulation, since AQP3-mediated water and glycerol transport have recently been involved in the migration and proliferation of epidermal keratinocytes and corneal reepithelialization in mammals (42).

Although the molecular mechanism(s) involved in the stimulation of development of embryos exposed to air and the role of FhAqp3 during gastrulation are yet unknown, we found that FhAqp3 both mRNA and protein levels were reduced in air-exposed embryos with respect to embryos continuously immersed in seawater. The physiological significance of this finding is intriguing although it may be speculated that this is part of the mechanism of the embryo to reduce evaporative water loss through the EVL, and/or to regulate the migration of blastomers, since gastrulation probably occurs at an increased rate in air-exposed embryos than in water-incubated embryos. These hypotheses however remain to be investigated, as well as the functional relationship of FhAqp3 with other aquaglyceroporins, such as Aqp7 and Aqp9, which may also be expressed during early embryogenesis, as shown in mammalian embryos (2, 17), and may play a role during dehydration resistance.

Perspectives

The data presented here demonstrate that *F. heteroclitus* embryos under laboratory-controlled conditions respond adaptively to environmental desiccation by accelerating development. Such a physiological process most likely evolved in this species as an adaptation for reproductive success in estuarine saltmarshes that are only flooded during the spring tides. Our observations indicate that, even though embryos are protected by a thickened chorion that possibly prevents evaporative

water loss, they are also able to transduce signals that detect environmental dehydration into molecular responses, leading to stimulation of growth and differentiation. One of the early responses seems to involve the downregulation of FhAqp3 during gastrulation. However, the precise role of FhAqp3 in gastrula embryos and the mechanisms controlling its expression still need to be elucidated. This study provides the critical first step for understanding the molecular basis underlying dehydration-stimulated embryonic development in *F. heteroclitus* and the potential role of FhAqp3.

ACKNOWLEDGMENTS

We thank J. M. Fortuño for technical assistance during scanning electron microscopy.

Present address for A. Tingaud-Sequeira: Génomique et Physiologie des Poissons, Université Bordeaux 1, UMR NuAGe, 33405 Talence, France.

GRANTS

This study was supported by the European Commission New and Emerging Science and Technologies (NEST) program (contract no. 012674-2 Sleeping Beauty) and by a grant from the Spanish Ministry of Education and Science (MEC; AGL2004-00316/ACU) to J. Cerdà. Participation of C. Zapater and F. Chauvigné was financed by a predoctoral fellowship from MEC (Spain) and by the European Commission [Marie Curie Research Training Network Aqua (glycero)porins, MRTN-CT-2006-035995], respectively.

REFERENCES

1. **Armstrong PB, Child JW.** Stages in the normal development of *Fundulus heteroclitus*. *Biol Bull* 128: 143–168, 1965.
2. **Barcroft LC, Offenberg H, Thomsen P, Watson AJ.** Aquaporin proteins in murine trophectoderm mediate transepithelial water movements during cavitation. *Dev Biol* 256: 342–354, 2003.
3. **Bayley M, Holmstrup M.** Water vapor absorption in arthropods by accumulation of myoinositol and glucose. *Science* 285: 1909–1911, 1999.
4. **Bigelow HB, Schroeder WC.** *Fishes of the Gulf of Maine.* US Fish and Wildlife Service, 1953.
5. **Broekhuyse RM, Kuhlmann ED, Stols AL.** Lens membranes. II. Isolation and characterization of the main intrinsic polypeptide (MIP) of bovine lens fiber membranes. *Exp Eye Res* 23: 365–371, 1976.
6. **Cerdà J, Calman BG, LaFleur GJ Jr, Limesand S.** Pattern of vitellogenesis and follicle maturational competence during the ovarian follicular cycle of *Fundulus heteroclitus*. *Gen Comp Endocrinol* 103: 24–35, 1996.
7. **Clegg JS.** Cryptobiosis—a peculiar state of biological organization. *Comp Biochem Physiol B Biochem Mol Biol* 128: 613–624, 2001.
8. **Cutler CP, Cramb G.** Branchial expression of an aquaporin 3 (AQP-3) homologue is downregulated in the European eel *Anguilla anguilla* following seawater acclimation. *J Exp Biol* 205: 2643–2651, 2002.
9. **Deen PM, Verdijk MA, Knoers NV, Wieringa B, Monnens LA, van Os CH, van Oost BA.** Requirement of human renal water channel aquaporin-2 for vasopressin-dependent concentration of urine. *Science* 264: 92–95, 1994.
10. **Denver RJ.** Environmental stress as a developmental cue: corticotropin-releasing hormone is a proximate mediator of adaptive phenotypic plasticity in amphibian metamorphosis. *Horm Behav* 31: 169–179, 1997.
11. **DiMichele L, Taylor MH.** The environmental control of hatching in *Fundulus heteroclitus*. *J Exp Zool* 214: 181–187, 1980.
12. **DiMichele L, Taylor MH.** The mechanism of hatching in *Fundulus heteroclitus*: development and physiology. *J Exp Zool* 217: 73–79, 1981.
13. **DiMichele L, Powers DA.** LDH-B genotype-specific hatching times of *Fundulus heteroclitus* embryos. *Nature* 296: 563–564, 1982.
14. **DiMichele L, Powers DA.** The relationship between oxygen consumption rate and hatching in *Fundulus heteroclitus*. *Physiol Zool* 57: 46–51, 1984a.
15. **DiMichele L, Powers DA.** Developmental and oxygen consumption rate differences between lactate dehydrogenase B genotypes of *Fundulus heteroclitus* and their effect on hatching time. *Physiol Zool* 57: 52–56, 1984b.
16. **Dunham PB, Cass A, Trinkaus JP, Bennett MVL.** Water permeability of *Fundulus* eggs. *Biol Bull* 139: 420–421, 1970.
17. **Edashige K, Tanaka M, Ichimaru N, Ota S, Yazawa K, Higashino Y, Sakamoto M, Yamaji Y, Kuwano T, Valdez DM Jr, Kleinhans FW, Kasai M.** Channel-dependent permeation of water and glycerol in mouse morulae. *Biol Reprod* 74: 625–632, 2006.
18. **Endeward V, Musa-Aziz R, Cooper GJ, Chen LM, Pelletier MF, Virkki LV, Supuran CT, King LS, Boron WF, Gros G.** Evidence that aquaporin 1 is a major pathway for CO_2 transport across the human erythrocyte membrane. *FASEB J* 20: 1974–1981, 2006.
19. **Fink RD, Cooper MS.** Apical membrane turnover is accelerated near cell-cell contacts in an embryonic epithelium. *Dev Biol* 174: 180–189, 1996.
20. **Fishman AP, Galante RJ, Winokur A, Pack AI.** Estivation in the African lungfish. *Proc Am Philos Soc* 136: 61–72, 1992.
21. **Froger A, Tallur B, Thomas D, Delamarche C.** Prediction of functional residues in water channels and related proteins. *Protein Sci* 7: 1458–1468, 1998.
22. **Giffard-Mena I, BouloV, Aujoulat F, Fowden H, Castille R, Charmantier G, Cramb G.** Aquaporin molecular characterization in the sea-bass (*Dicentrarchus labrax*): the effect of salinity on AQP1 and AQP3 expression. *Comp Biochem Physiol Part A Mol Integr Physiol* 148: 430–444, 2007.
23. **Gutierrez-Estrada JC, Prenda J, Oliva F, Fernández-Delgado C.** Distribution and habitat preferences of the introduced mummichog *Fundulus heteroclitus* (Linneaus) in South-western Spain. *Est Coastal Shelf Sci* 46: 827–835, 1998.
24. **Hara-Chikuma M, Verkman AS.** Roles of aquaporin-3 in the epidermis. *J Invest Dermatol* 128: 2145–2151, 2008.
25. **Hsiao SM, Meier AH.** Comparison of semilunar cycles of spawning activity in *Fundulus grandis* and *F. heteroclitus* held under constant laboratory conditions. *J Exp Zool* 252: 213–218, 1989.
26. **Hsiao SM, Greeley MS, Wallace RA.** Reproductive cycling in female *Fundulus heteroclitus*. *Biol Bull* 186: 217–281, 1994.
27. **Hsiao SM, Limesand SW, Wallace RA.** Semilunar follicular cycle of an intertidal fish: the *Fundulus* model. *Biol Reprod* 54: 809–18, 1996.
28. **Jones S.** On the occurrence of diapause in the eggs of Indian cyprinodonts. *Curr Sci Bangalore* 13: 1–7-108, 1944.
29. **Kaighn ME.** A biochemical study of the hatching process in *Fundulus heteroclitus*. *Dev Biol* 9: 56–80, 1964.
30. **Kao CY, Chambers R, Chambers EL.** Internal hydrostatic pressure of the *Fundulus* egg. II. Permeability of the chorion. *J Cell Physiol* 44: 447–461, 1954.
31. **King LS, Kozono D, Agre P.** From structure to disease: the evolving tale of aquaporin biology. *Nat Rev Mol Cell Biol* 5: 687–698, 2004.
32. **Laemmli UK.** Cleavage of structural proteins during the assembly of the head of bacteriophage T4. *Nature* 227: 680–685, 1970.
33. **Lee DS, Gilbert CR, Hocutt VH, Jenkins RE, McAllister DC, Stauffer JR.** *Atlas of North American Freshwater Fishes*. Publication of the North Carolina Biological Survey No. 1980-12. Raleigh, NC: North Carolina Museum of Natural Sciences, 1980.
34. **Livak KJ, Schmittgen TD.** Analysis of relative gene expression data using real-time quantitative PCR and the $2^{-\Delta\Delta Ct}$ method. *Methods* 25: 402–408, 2001.
35. **Machado BE, Podrabsky JE.** Salinity tolerance in diapausing embryos of the annual killifish *Austrofundulus limnaeus* is supported by exceptionally low water and ion permeability. *J Comp Physiol [B]* 177: 809–820, 2007.
36. **Mathias RT, Rae JL, Baldo GJ.** Physiological properties of the normal lens. *Physiol Rev* 77: 21–50, 1997.
37. **Mayhew WW.** Adaptations of the amphibian, *Scaphiopus couchi*, to desert conditions. *Am Mid Nat* 74: 95–109, 1965.
38. **Mead RA.** Embryonic diapause in vertebrates. *J Exp Zool* 266: 629–641, 1993.
39. **Myers GS.** Studies on South American fresh-water fishes. *Stanford Ichth Bull* 2: 89–114, 1942.
40. **Nielsen S, Smith BL, Christensen EI, Agre P.** Distribution of the aquaporin CHIP in secretory and resorptive epithelia and capillary endothelia. *Proc Natl Acad Sci USA* 90: 7275–7279, 1993.
41. **O'Boyle S, Bree RT, McLoughlin S, Grealy M, Byrnes L.** Identification of zygotic genes expressed at the midblastula transition in zebrafish. *Biochem Biophys Res Commun* 358: 462–468, 2007.
42. **Papadopoulos MC, Saadoun S, Verkman AS.** Aquaporins and cell migration. *Pflügers Arch* 456: 693–700, 2008.
43. **Podrabsky JE, Hand SC.** The bioenergetics of embryonic diapause in an annual killifish, *Austrofundulus limnaeus*. *J Exp Biol* 202: 2567–2580, 1999.

44. **Podrabsky JE, Hand SC.** Depression of protein synthesis during diapause in embryos of the annual killifish *Austrofundulus limnaeus*. *Physiol Biochem Zool* 73: 799–808, 2000.
45. **Podrabsky JE, Carpenter JF, Hand SC.** Survival of water stress in annual fish embryos: dehydration avoidance and egg envelope amyloid fibers. *Am J Physiol Regul Integr Comp Physiol* 280: R123–R131, 2001.
46. **Podrabsky JE, Lopez JP, Fan TW, Higashi R, Somero GN.** Extreme anoxia tolerance in embryos of the annual killifish *Austrofundulus limnaeus*: insights from a metabolomics analysis. *J Exp Biol* 210: 2253–2266, 2007.
47. **Powers DA, Lauerman T, Crawford D, DiMichele L.** Genetic mechanisms for adapting to a changing environment. *Annu Rev Genet* 25: 629–659, 1991.
48. **Preston GM, Carroll TP, Guggino WB, Agre P.** Appearance of water channels in *Xenopus* oocytes expressing cell CHIP28 protein. *Science* 256: 385–387, 1992.
49. **Preston GM, Jung JS, Guggino WB, Agre P.** The mercury-sensitive residue at cysteine 189 in the CHIP28 water channel. *J Biol Chem* 268: 17–20, 1993.
50. **Randall JE.** Introductions of marine fishes to the Hawaiian Islands. *Bull Mar Sci* 41: 490–502, 1987.
51. **Rohde LA, Heisenberg CP.** Zebrafish gastrulation: cell movements, signals, mechanisms. *Int Rev Cytol* 261: 159–192, 2007.
52. **Scott WB, Crossman EJ.** *Freshwater Fishes of Canada*. Oakville, Canada: Galt House, 1998.
53. **Seale A.** The successful transference of black bass into the Philippine Islands with notes on the transportation of live fish long distances. *Philippine J Sci* 5: 153–159, 1910.
54. **Shanklin DR.** Studies on the *Fundulus* chorion. *J Cell Comp Physiol* 53: 1–11, 1959.
55. **Sugiyama H, Murata K, Iuchi I, Yamagami K.** Evaluation of solubilizing methods of the egg envelope of the fish, *Oryzias latipes*, and partial determination of amino acid sequence of its subunit protein, ZI-3. *Comp Biochem Physiol B Biochem Mol Biol* 114: 27–33, 1996.
56. **Sui H, Han BG, Lee JK, Walian P, Jap BK.** Structural basis of water-specific transport through the AQP1 water channel. *Nature* 414: 872–878, 2001.
57. **Taylor MH.** Environmental and endocrine influences on reproduction of *Fundulus heteroclitus*. *Am Zool* 26: 159–171, 1986.
58. **Taylor MH.** Entrainment of the semilunar reproductive cycle of *Fundulus heteroclitus*. *Proc 4th Int Symp Reproductive Physiology of Fish, Sheffield, FishSymp 91,* 157–159, 1991.
59. **Taylor MH.** A suite of adaptations for intertidal spawning. *Am Zool* 39: 313–320, 1999.
60. **Taylor MH, DiMichele L.** Spawning site utilization in a Delaware population of *Fundulus heteroclitus* (Pisces: Cyprinodontidae). *Copeia* 3: 719–725, 1983.
61. **Taylor MH, DiMichele L, Leach GJ.** Egg stranding in the life cycle of the mummichog, *Fundulus heteroclitus*. *Copeia* 2: 397–399, 1977.
62. **Taylor MH, Leach GJ, DiMichele L, Levitan WM, Jacob WF.** Lunar spawning cycle in the mummichog, Fundulus heteroclitus (Pisces: Cyprinodontidae). *Copeia* 291–297, 1979.
63. **Thisse B.** Expression of the zebrafish genome during embryogenesis (NIH R01 RR15402). *ZFIN Direct Data Submission*, 2001.
64. **Tingaud-Sequeira A, Cerdà J.** Phylogenetic relationships and gene expression pattern of three different cathepsin L (Ctsl) isoforms in zebrafish: Ctsla is the putative yolk processing enzyme. *Gene* 386: 98–106, 2007.
65. **Tingaud-Sequeira A, Chauvigné F, Fabra M, Lozano J, Raldúa D, Cerdà J.** Structural and functional divergence of two fish aquaporin-1 water channels following teleost-specific gene duplication. *BMC Evol Biol* 8: 259, 2008.
66. **Trinkaus JP.** Ingression during early gastrulation of *Fundulus*. *Dev Biol* 177: 356–370, 1996.
67. **Verkman AS, Ives HE.** Water permeability and fluidity of renal basolateral membranes. *Am J Physiol Renal Fluid Electrolyte Physiol* 250: F633–F643, 1986.
68. **Virkki LV, Cooper GJ, Boron WF.** Cloning and functional expression of an MIP (AQP0) homolog from killifish (*Fundulus heteroclitus*) lens. *Am J Physiol Regul Integr Comp Physiol* 281: R1994–R2003, 2001.
69. **Withers PC, Guppy M.** Do Australian desert frogs co-accumulate counteracting solutes with urea during aestivation? *J Exp Biol* 199: 1809–1816, 1996.
70. **Wourms JP.** The developmental biology of annual fishes. III. Pre-embryonic and embryonic diapause of variable duration in the eggs of annual fishes. *J Exp Zool* 182: 389–414, 1972.